Lab 07: Active Filter Circuits

Arturo Salinas-Aguayo

ECE 2001 Electrical Circuits

Dr. David J. Giblin, Section 331.660.701.810-1253

Mechanical Engineering Department

College of Engineering, University of Connecticut

Coded in LaTeX

Contents

1 Abstract

This experimental work builds greatly upon the previous work employed in experiment 6. The big limitation to passive filters is that they can only produce a gain up to 1. Passive elements cannot add energy to a system. This week's work takes this into consideration by reintroducing circuits with the LM741 op-amp.

First, a low pass filter is built, then by simply changing the ordering of the passive components around the op amp, a high pass filter is constructed. Lastly, the elementary task of designing a filter is introduced around designing and building a multiple-feed bandpass filter.

2 Introduction

The main characteristics of active filters aim to augment the passive filter response which had three main limitations: a max fixed gain factor of 1, the need for big and bulky inductors, and their poor response below the audio frequency range.

Active filters, however, employ combinations of resistors, capacitors, and op amps. They are smaller and less expensive because they do not require the use of coils (inductors). This opens the doors for many different advanced applications such as shipboard use (an application I have extensive experience with). Second, they can provide an amplification gain in addition to the frequency response exhibited in the passive versions of the RLC filters. Finally, they can be integrated with buffer amplifiers to isolate each stage of a filter such that the subsequent stages do not load the previous stage with impedance.

From the published paper, *A Practical Method of Designing RC Active Filters* by R. P. Sallen and E. L. Key, a primary application of these filters is such that the frequency range below 30 cps is particularly not suited to allow the design of RLC circuits. This comes into play with applications such as the source range neutron detectors in the nuclear industry.

These detectors must be able to detect the faintest amount of neutron flux in order to properly allow the operators to safely bring a reactor from a subcritical shutdown state to supercriticality in a slow, controlled fashion. When a reactor has been shut down a long time, the fuel is essentially dormant in something called the fiducial state. Because of this, starting up a reactor for the first time in its life or after a long shutdown period (on the order of half a year or more) is particularly difficult to do, as source range detectors need to be able to read power at very low frequencies to prevent exceedingly high startup rates which would lead to prompt criticality.

Thanks to the work published by these gentlemen, filters were able to be implemented in the first nuclear submarine, the USS *Nautilus*, in her S1B nuclear power plant. Very cutting edge for the time.

Looking forward on this concept, this allows the design of each stage independently in order to create a cascaded effect similar to Design Project 1, but this time with much less noise. For now though, the active filter is explored and modeled in SPICE simulation as well as realized in hardware.

Note: All 15 nF capacitors are substituted with 22 nF capacitors due to hardware availability in the experiment kit.

3 Theory

3.1 The Sallen–Key Filter

The circuits built are all minimal 2-pole active filters named after their primary investigators at MIT in 1955, R. P. Sallen and E. L. Key. The original research employed an op amp with a particular arrangement of resistors and capacitors, allowing different filter characteristics (low-pass, high-pass, bandpass) by interchanging the positions of these passive components. Figure 1 shows the generic Sallen–Key topology.

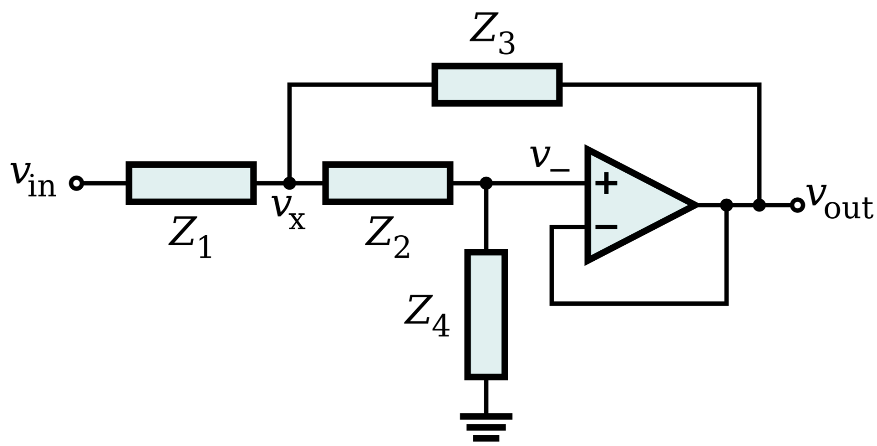

Figure 1: Generic Sallen–Key Filter Topology

3.2 Low-Pass Sallen–Key Filter

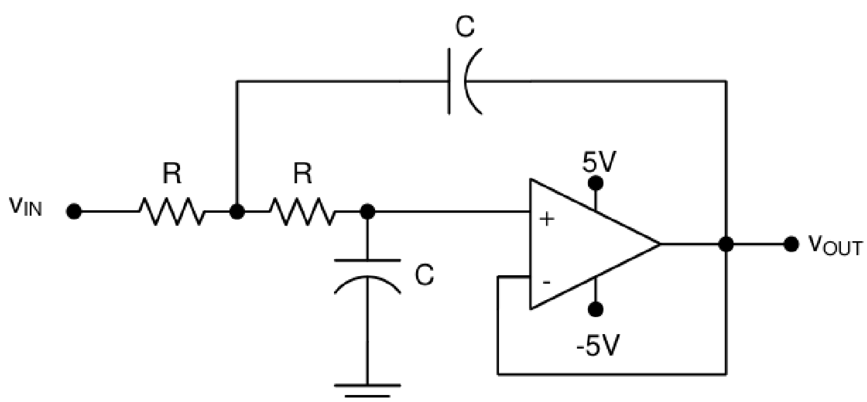

Figure 2: Circuit One: Sallen–Key Low-Pass Filter.

In its low-pass form, the filter places two RC branches in the negative feedback loop of the op amp. A well-known second-order unity-gain transfer function is: $(s = j\omega)$

$$H = \frac{1}{s^2R^2C^2 + 2sRC + 1}$$

yielding a cutoff or corner frequency

$$f_c \; = \; \frac{1}{2\pi\, R\, C}.$$

Because it is a two-pole filter, it exhibits a $-40\,\mathrm{dB/decade}$ roll-off in the stopband and has a flatter passband than a comparable first-order filter.

3.3 High-Pass Sallen–Key Filter

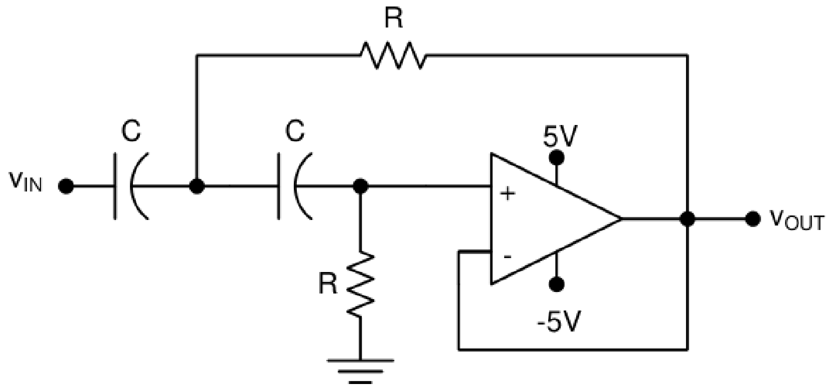

Figure 3: Circuit Two: Sallen–Key High-Pass Filter.

The high-pass configuration swaps the resistor and capacitor placements. Its transfer function is: $(s = j\omega)$

$$H = \frac{-s^2R^2C^2}{s^2R^2C^2 + 2sRC + 1}$$

with the same nominal cutoff frequency

$$f_c \;=\; \frac{1}{2\pi\,R\,C}.$$

Ideally, it provides negligible gain at low frequencies and passes higher-frequency components. However, this circuit will not behave only like a high pass filter, because once the reactive capacitor gets a certain high frequency, the capacitor will begin to act like a short circuit, and the op amp will effectively be open-loop. This is evident in the data in Figure 6.

3.4 Multiple-Feedback (MFB) Bandpass Filter

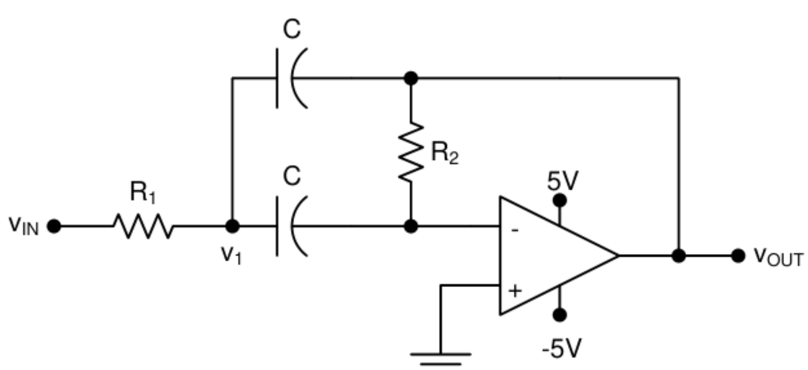

Figure 4: Circuit Three: Multiple-Feedback Bandpass Filter.

The MFB bandpass filter is another second-order topology but arranges two resistors and two capacitors in a specific feedback loop. The transfer function can be derived using the node voltage method as such: $(s = j\omega)$

$$H(s) = \frac{-sR_2C}{s^2R_1R_2C^2 + 2sR_1C + 1}$$

which may be rewritten to match a standard second-order bandpass form:

$$f_0 = \frac{1}{2\pi, C\sqrt{R_1R_2}}$$
$$A_r = -\frac{R_2}{2R_1}$$
$$Q = \frac{1}{2}\sqrt{\frac{R_2}{R_1}}$$

By choosing R_1, R_2, and C, one can specify the center frequency f_0 and quality factor Q. Because the peak amplitude occurs at f_0, we say the bandwidth BW is bounded by the $-3\,\mathrm{dB}$ frequencies, and for a standard bandpass $Q = \frac{f_0}{\mathrm{BW}}$.

4 Experimental Procedures

4.1 Circuit One: Sallen–Key Low-Pass Filter

Referring to Figure 2, the expected cutoff frequency is

$$f_c = \frac{1}{2\pi\,RC} = \frac{1}{2\pi \cdot 1000 \cdot (22 \times 10^{-9})} \approx 7234.32\,\mathrm{Hz}.$$

The ADALM2000 and Scopy software was used in conjunction with the Network Analyzer tool in order to scan the same frequency range simulated in SPICE.

4.2 Circuit Two: Sallen–Key High-Pass Filter

The high-pass version is constructed by simply interchanging the resistor and capacitor placements.

$$R = 1k\Omega, \quad C = 22nF.$$

The nominal cutoff is the same ($\approx 7.2kHz$) as Circuit One.

4.3 Circuit Three: Multiple-Feedback Bandpass Filter

A bandpass filter with center frequency near 12 kHz and $Q \approx 0.4$ was designed using:

$$R_1 = 47\,\mathrm{k\Omega}, \quad R_2 = 30\,\mathrm{k\Omega}, \quad C = 330\,\mathrm{pF}.$$

To achieve a quality factor of 0.4, we require

$$0.4 = \frac{1}{2}\sqrt{\frac{R_2}{R_1}} \implies \frac{R_2}{R_1} = 0.64$$

This can be achieved with the standard resistor values of:

$$R_1 = 47k\Omega$$
$$R_2 = 30k\Omega$$

Then, to achieve a center frequency of $12kHz$, the following calculation is made:

$$12kHz = \frac{1}{2\pi, C\sqrt{R_1 R_2}} \implies C = 353.2pF$$

The closest standard size capacitor is $330pF$. See Figure 4 for the amplitude response.

5 Results and Discussion

5.1 Sallen–Key Low-Pass Filter

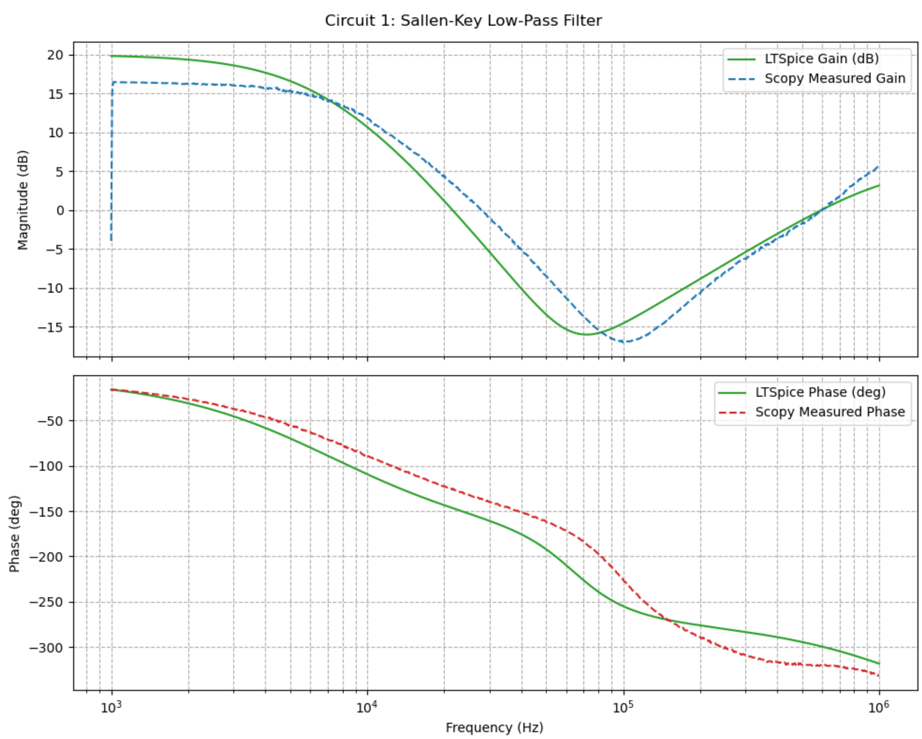

Figure 5: Bode plot of Circuit One (Sallen–Key Low-Pass).

Figure 5 shows the comparison between the measured response (blue dashed line) and the LTspice simulation (green line) for the low-pass filter. The measured cutoff frequency is close to the theoretical $\sim 7.2\,\text{kHz}$. Below $1\,\text{kHz}$, the passband gain is near unity (or about $0\,\text{dB}$), agreeing well with the simulation. As frequency increases beyond f_c, the filter attenuates at roughly $-40\,\text{dB/decade}$.

Freq (Hz)	Gain (dB)	Phase (°)
1000.00	-60.326	163.941
2781.14	-23.818	143.144
7734.71	-9.505	101.996
21511.30	-2.699	46.583
59825.80	-7.910	-18.496
167152.00	-15.162	-33.234
464872.00	-20.953	-7.757
1292870.00	-6.922	26.915
3595650.00	-5.339	-29.016
10000000.00	-10.155	-48.947

Table 1: Circuit One: Sallen–Key Low-Pass Filter (Full Sweep)

Nevertheless, the overall agreement is good. The phase plot also shows consistent behavior, with minor deviations above $\sim 100\,\text{kHz}$.

5.2 Sallen–Key High-Pass Filter

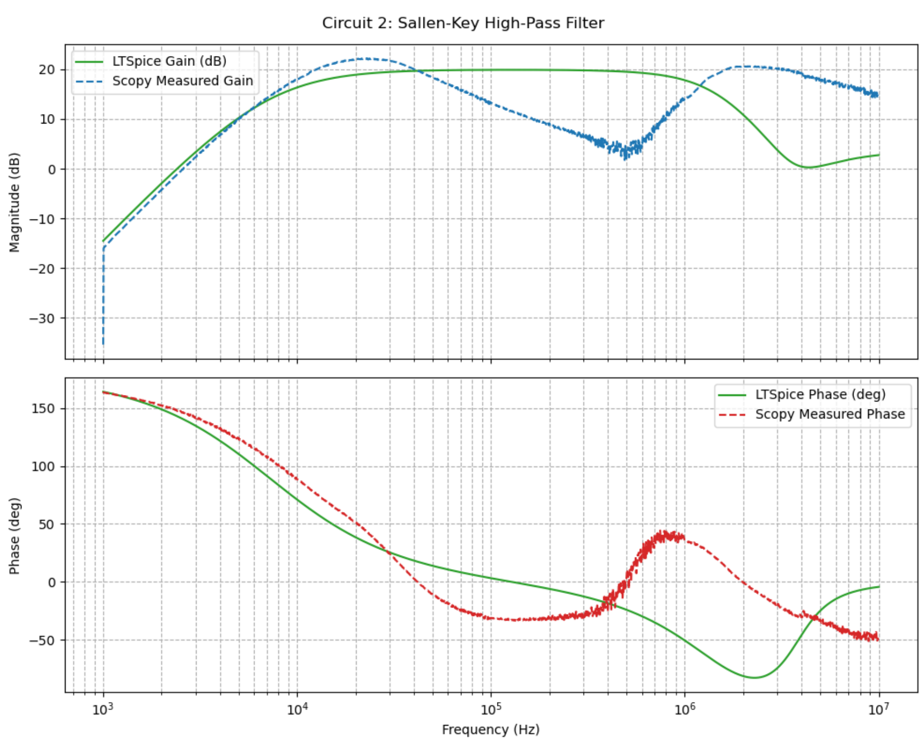

Figure 6: Bode plot of Circuit Two (Sallen–Key High-Pass).

Figure 6 shows the high-pass filter's amplitude and phase responses. Theoretically, it should attenuate signals below 7.2 kHz and approach unity gain at higher frequencies. While the

Additionally, the measured data shows a mild passband peaking above 1 MHz, once the capacitor in the feedback loop becomes over-excited with the input frequency.

Freq (Hz)	**Gain (dB)**	**Phase (°)**
1000.00	-22.093	-11.131
2782.56	-2.011	-30.668
7742.64	-4.424	-71.028
21544.30	-14.624	-121.834
59948.40	-29.426	-167.256
166810.00	-30.978	-274.000
464159.00	-20.523	-314.000
1291550.00	-10.420	-336.000
3593810.00	-8.838	-21.137
10000000.00	-13.055	-46.393

Table 2: Circuit Two: Sallen–Key High-Pass Filter (Full Sweep)

Despite these high-frequency differences, the high-pass nature of the filter is clearly evident: low-frequency signals are heavily attenuated, and signals above roughly 7 kHz see a near-constant passband gain. This makes it appear to be a band-pass filter above this frequency range.

5.3 Multiple-Feedback Bandpass Filter

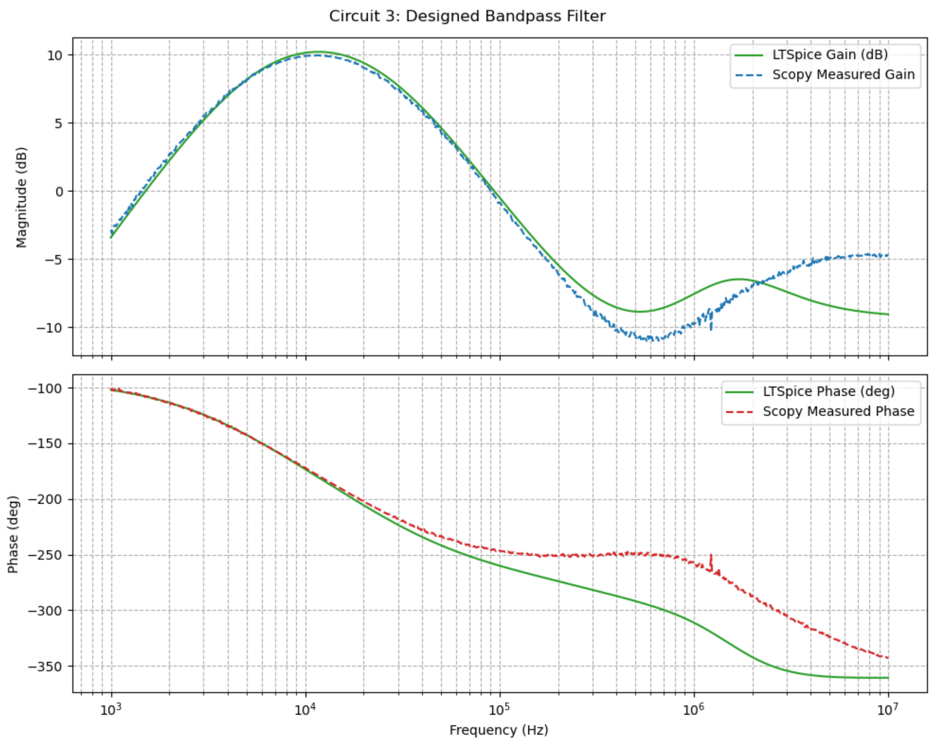

Figure 7: Bode plot of Circuit Three (MFB Bandpass).

Figure 7 compares the measured bandpass response with the LTspice results. A clear peak is near $\sim 11.5\,\text{kHz}$, slightly below the theoretical design of $12\,\text{kHz}$. The cutoff frequencies are approximately:

$$f_H = 36.5KHz$$
$$f_L = 4.47KHz$$

This produces a bandwidth of

$$BW = 36.5KHz - 4.47KHz = 32.03KHz.$$

The ratio of the center frequency to the bandwidth is:

$$Q = \frac{f_0}{BW} = \frac{11.5KHz}{32.03KHz} \approx 0.359.$$

This aligns with the theoretical design characteristics within tolerances of $\pm 10\%$.

Freq (Hz)	Gain (dB)	Phase (°)
100.00	-41.052	-99.186
359.38	-31.464	-99.591
1291.55	-20.947	-108.060
4641.59	-12.018	-141.522
16681.00	-10.191	163.425
59948.40	-16.650	120.627
215443.00	-26.198	106.359
774264.00	-30.120	106.507
2782560.00	-26.087	-55.487
10000000.00	-24.548	14.758

Table 3: Circuit Three: Multiple-Feedback Bandpass Filter

In summary, the MFB bandpass filter demonstrates the expected peaked response around the design frequency. The measured phase response also closely matches the simulation at low to mid frequencies, with additional discrepancy at higher frequencies due to the non-ideal nature of the LM741.

6 Conclusion

Through both theoretical derivation and LTspice simulation, approximate cutoff (or center) frequencies were established, and then measured the actual frequency response of each filter using the Network Analyzer in Scopy.

- **Sallen–Key Low-Pass:**
  The measured cutoff frequency closely matched the theoretical value ($\sim 7.2\,\text{kHz}$), and the roll-off slope of $-40\,\text{dB/decade}$ was evident. Minor high-frequency discrepancies were consistent with the op amp's limited bandwidth.

- **Sallen–Key High-Pass:**
  Good overall agreement in the passband and near the cutoff, although at low frequencies, a small DC offset appeared, demonstrating that real filters do not have a perfectly zero gain at DC. The high-pass nature was still clear, attenuating low frequencies significantly. At high frequencies, the filter fails to act as the reactive portions of the feedback loop take over, giving the output a band-pass like characteristic.

- **MFB Bandpass Filter:**
  The center frequency measured around $11.5\,\text{kHz}$, close to the designed $12\,\text{kHz}$. The measured quality factor was in reasonable agreement with the theory, demonstrating how component tolerances and op amp non-idealities can slightly shift the response. The phase characteristics tracked the simulation below $100\,\text{kHz}$, but diverged somewhat at higher frequencies.

Overall, these experiments highlight the strengths of second-order active filters (such as the sharper roll-off vs. first-order, and ease of tuning). This provides a solid ground for the upcoming final design project.